

# Rolled up or crumpled: phases of asymmetric tethered membranes

Tirthankar Banerjee,<sup>1,2,\*</sup> Niladri Sarkar,<sup>3,4,†</sup> John Toner,<sup>5,‡</sup> and Abhik Basu<sup>2,3,§</sup>

<sup>1</sup>LPTMS, UMR 8626, CNRS, Univ. Paris-Sud,

Université Paris-Saclay, 91405 Orsay CEDEX, France

<sup>2</sup>Condensed Matter Physics Division, Saha Institute of Nuclear Physics,  
1/AF Bidhannagar, Calcutta 700064, West Bengal, India

<sup>3</sup>Max-Planck Institut für Physik Komplexer Systeme, Nöthnitzer Str. 38, 01187 Dresden, Germany

<sup>4</sup>Laboratoire Physico Chimie Curie, UMR 168, Institut Curie,  
PSL Research University, CNRS, Sorbonne Université, 75005 Paris, France.

<sup>5</sup>Department of Physics and Institute of Theoretical Science,  
University of Oregon, Eugene, Oregon 97403, USA

(Dated: March 17, 2022)

We show that inversion-asymmetric tethered membranes exhibit a new double-spiral phase with long range orientational order not present in symmetric membranes. We calculate the universal algebraic spiral shapes of these membranes in this phase. Asymmetry can trigger the crumpling of these membranes as well. In-vitro experiments on lipid, red blood cell membrane extracts, and on graphene coated on one side, could test these predictions.

The statistical mechanics of membranes has long generated considerable theoretical and experimental interest [1]. In contrast to linear polymers [2, 3], fluctuating surfaces can exhibit a wide variety of different phases, depending on rigidity, surface tension, and topology. Polymerized, or “tethered” membranes [1, 4] are two-dimensional (2D) analogs of linear polymer chains. But, unlike polymers, which are always coiled up, tethered membranes are known [1, 5] to display a statistically flat phase with long range orientational order (LRO) in the surface normals. The very existence of a 2D flat phase is surprising, since the well-known Hohenberg-Mermin-Wagner theorem (HMWT) forbids spontaneous symmetry breaking for 2D systems with a continuous symmetry [6, 7]. Membranes get around this theorem via the coupling between in-plane elastic degrees of freedom and out-of-plane undulations, which introduces an effective long-ranged interaction between those undulation modes.

Most studies of tethered membranes have considered only *inversion-symmetric* membranes, i.e., membranes that are identical on both sides. Many real membranes, e.g., graphene coated on one side by some substance (e.g., polymer or a layer of lipid), *in-vivo* red blood cell membranes and *in-vitro* spectrin-deposited model lipid bilayers [8] are *structurally inversion asymmetric*. The effects of such asymmetry are still largely unexplored.

In this Letter, we investigate the effects of asymmetry, and develop a generic and experimentally testable theory of equilibrium asymmetric tethered membranes (ATMs). We find that such membranes exhibit a new, “spiral state” not found in symmetric membranes. As illustrated in Fig. 1, the mean spatial configuration of this state can be obtained by joining two coplanar spirals of opposite handedness at their base, and extruding that curve in the direction perpendicular to the plane of the spirals. Note that this state, like the flat phase of symmetric membranes, exhibits long-ranged orienta-

tional order (LRO), although, obviously, it has a very different structure.

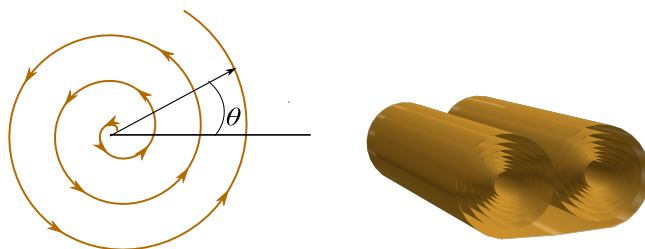


FIG. 1. (Color online)(left) Schematic diagram of the cross section of one of the double spirals, (right) Schematic diagram of a double spiral structure of our model membrane.

In the spiral state at temperature  $T = 0$ , all ATMs assume the same shape. This is also true at  $T \neq 0$ , although the shape differs from that at  $T = 0$ ; in a sense, the  $T \neq 0$  shape is *infinitely* thermally expanded relative to the  $T = 0$  configuration. The  $T = 0$  configuration is, for large  $L_m$ , simply a double spiral of Archimedes, each with a hole in the center; i.e., in polar coordinates, each spiral is given by

$$r(\theta) = r_0 + a \frac{\theta}{2\pi}; \quad (1)$$

see Fig. 1 (right). In equation (1),  $a$  is the thickness of the membrane,  $\theta = 0$  corresponds to the inner edge of the membrane, and  $r_0$  is the radius of the hole at the center of each spiral. Choosing this form for  $r(\theta)$  simply means that the membrane is curled up as tightly as it can, given excluded volume effects.

Thermal fluctuations considerably change this picture, opening up the spiral into the form:

$$r(\theta) = R_0 \theta^\beta, \quad (2)$$

where the universal exponent  $\beta$  is related to the equally universal exponent  $\eta$  characterizing the anomalous bend

elasticity [1] of *symmetric* membranes through the relation  $\beta = \frac{4}{2+\eta} \approx 4 - \frac{2}{3}\sqrt{15} \approx 1.418$ . The numerical estimate is based on the theoretical estimate  $\eta = 4/(1 + \sqrt{15}) \approx 0.821$  obtained by Radzihovsky and LeDousal [9]. In addition, the scale length  $R_0$  exhibits universal scaling with temperature and membrane parameters, which can also be related exactly to the exponent  $\eta$ ; in particular, we find

$$R_0 \propto T^{2(2-\eta)/(2+\eta)} \approx T^{0.836}. \quad (3)$$

The total radius  $R_T$  of the spiral regions also exhibits universal scaling, in this case with the spatial extent  $L_m$  of the membrane:

$$R_T = R_0^{1-\alpha} L_m^\alpha, \quad \alpha \equiv \frac{4}{6+\eta} \approx 0.586. \quad (4)$$

Increasing asymmetry eventually induces a novel structural instability which actually crumples the membrane [1, 10]. In further contrast with symmetric membranes, we find two distinct regimes of parameter space within the crumpled phase of ATMs. In one of these, (hereafter called “strongly crumpled”, or “SC”), the membrane will be crumpled no matter how small it is, while in the second (hereafter called “weakly crumpled” or “WC”), it is only crumpled if its lateral spatial extent  $L_m$  exceeds a critical size  $L_c$ , which depends on material parameters of the membrane. Smaller membranes (i.e.,  $L_m < L_c$ ) exhibit a spiral structure similar to that found in the spiral phase, but different in its scaling properties. Those scaling properties can be obtained from those specified by equations (2), (3) and (4) by replacing  $\eta$  everywhere it appears by 0. This crumpling behavior is summarized in Fig. 2, in which  $\chi$  is a phenomenological parameter (defined in equation (5) below) characterizing the asymmetry of the membrane, with  $\chi = 0$  for symmetrical membranes.

We will now outline the derivation of these results; more detail is given in the associated long paper (ALP) [11].

We begin by formulating the elastic model for a single turn of the spiral structure, on length scales short compared to both the local radius of curvature  $R$  and the typical distance  $L_H$  between successive points of contact between that turn and the turns immediately inside and outside of it. A membrane patch of linear size  $L \ll L_H$  behaves like an isolated, free membrane with no contact with anything else. The results of this analysis will then be used as inputs to treat the membrane on progressively larger scales: first, to compute  $L_H$ , and thereby calculate the interaction between successive turns of the membrane, and then on length scales comparable to  $R$ , to calculate the large scale spiral structure of the membrane.

For  $L \ll L_H$  and  $L \ll R$ , we can describe the membrane by a single-valued field  $h(\mathbf{r})$  in the Monge gauge and lateral displacement by a 2D vector field  $\mathbf{u}(\mathbf{r})$  [1, 12].

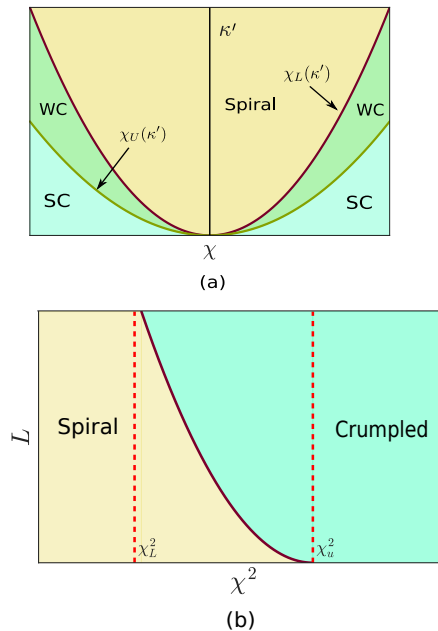


FIG. 2. (Color online) (a) Schematic “phase diagram” in the  $\chi^2 - \kappa'$  plane. (b) Schematic “phase diagram” in the  $\chi^2 - L$  plane for fixed  $\kappa$ . The continuous curve (black) is the line  $L = \xi(\chi^2)$ , demarcating the spiral and crumpled phases.

General symmetry considerations then dictate the following form for the free energy functional  $F$  for elastically isotropic (i.e., either amorphous or hexagonal crystalline), tensionless asymmetric tethered membranes:

$$F = \frac{1}{2} \int d^2r [\kappa'(\nabla^2 h)^2 + \lambda u_{ii}^2 + 2\mu u_{ij}u_{ij} + 2\chi u_{ii}\nabla^2 h] + \int d^2r C\nabla^2 h \quad (5)$$

to leading order in gradients; here  $r = |\mathbf{r}|$ ,  $\mathbf{r} = (x, y)$  with  $(\mathbf{r}, h)$  denoting the coordinate of a point on the membrane in the three-dimensional embedding space. The strain tensor  $u_{ij} = \frac{1}{2}(\nabla_i u_j + \nabla_j u_i + \nabla_i h \nabla_j h)$ , ignoring irrelevant terms, and  $\nabla^2 h$  is approximately the mean curvature for nearly flat membranes. This model (5) differs from the model for symmetric membranes [1, 12, 13] by the addition of two generic inversion-symmetry breaking terms: a linear “spontaneous curvature” term  $C\nabla^2 h$ , that makes the membrane want to curl up with a radius of curvature  $R_s \propto 1/C$  and a term  $\chi u_{ii}\nabla^2 h$ , that favors local bending of the membrane in response to local compression of the elastic network. See Ref. [14] for a term analogous to our  $\chi$  term introduced for *fluid* membranes.

Working to quadratic order in the fields, and integrating over  $\mathbf{u}$ , gives an effective free energy functional that depends only on  $h(\mathbf{r})$ :

$$\mathcal{F}_{eff} = \int \frac{d^2r}{(2\pi)^2} \left[ \frac{\kappa_0}{2} (\nabla^2 h)^2 + C\nabla^2 h \right], \quad (6)$$

with an effective bending modulus  $\kappa$ :

$$\kappa_0 = \kappa' - \frac{\chi^2}{2\mu + \lambda} \equiv \kappa'(1 - \chi^2/\chi_U^2), \quad (7)$$

where we have defined

$$\chi_U^2 = \kappa'(2\mu + \lambda). \quad (8)$$

Evidently,  $\kappa_0 < \kappa'$ . Thermodynamic stability of the membrane clearly requires  $\kappa_0 > 0$ , otherwise instability ensues. This implies that  $\chi_U^2$  is an instability threshold for  $\chi^2$ , with larger  $\chi^2$ 's being unstable. This is the asymmetry-induced crumpling discussed earlier in this Letter, which we see can occur even at  $T = 0$ . Since (7) is  $q$ -independent, any ensuing crumpling takes place at *all scales*, meaning an arbitrarily small membrane will be crumpled, provided  $\kappa_0 < 0$ . We will see later that anharmonic effects actually cause the membrane to crumple for a larger range of  $\chi$ 's; specifically, when  $\chi^2 > \chi_L^2$ , although for  $\chi_L^2 < \chi^2 < \chi_U^2$ , crumpling only occurs if the membrane is sufficiently large.

We now turn to the uncrumpled case  $\kappa_0 > 0$ , and show that the ground state structure is the double spiral of Archimedes illustrated in Fig. 1. Since  $\mathcal{F}$  is bilinear in  $u_i$ , we can follow [1] and integrate *exactly* over  $u_i$  in calculating the partition function associated with (5) to arrive at an effective free energy  $F_h$  that depends only on  $h$  (now including anharmonic terms in  $h$ ). The result, given in detail in the ALP, is a model with the same long ranged interaction between Gaussian curvatures as in symmetric tethered membranes [1], and a new, weaker, but still long-ranged, interaction between Gaussian and mean curvature  $\nabla^2 h$  that is unique to asymmetric membranes, where the local Gaussian curvature is given approximately by  $G(\mathbf{r}) \approx (\partial_x^2 h)(\partial_y^2 h) - (\partial_x \partial_y h)^2$  for nearly flat membranes. This long-ranged interaction between Gaussian curvatures  $G(\mathbf{r})$  at different points suppresses Gaussian curvature, causing the membrane to curl in only one direction in the spiral state.

In the ALP, we show that the long-ranged interactions between the mean and the Gaussian curvature do not alter this conclusion.

We will now more precisely determine the shape of the membrane at  $T = 0$ . Minimizing (6) over the mean inverse radius of curvature  $\nabla^2 h$  implies that the membrane energetically prefers to curl up with  $\nabla^2 h = \frac{1}{R_1} = -\frac{C}{\kappa_0} \equiv -\frac{1}{R_s}$ , where we have defined the spontaneous radius of curvature  $R_s = \frac{\kappa_0}{C}$ . However, a membrane of lateral extent  $L > \frac{\pi R_s^2}{a}$ , where  $a$  is the thickness of the membrane, cannot fit into a cylinder of radius  $R_s$ , because its total volume  $L^2 a$  will be greater than the volume of a cylinder of radius  $R_s$  and length  $L$ . Therefore, the best the membrane can do is to curl up as tightly as it can without overlapping itself. The shape that accomplishes this while bending in only one direction is the double spiral of Archimedes described by (1). The reason *two* spirals

form is that by so doing the membrane can reduce the average value of  $R_1$ , since each spiral only has to wind out  $\frac{1}{\sqrt{2}}$  as far.

As in symmetric membranes [1, 12, 13], at non-zero temperatures, the combination of thermal fluctuations and anharmonic effects substantially modify the behavior of the membrane. To study this, we perform a perturbative renormalization group (RG) analysis of the model (5), which we remind the reader is only valid on length scales  $L \ll L_H$ . As usual, the RG is done by tracing over the short wavelength Fourier modes of  $h(\mathbf{r})$ , followed by a rescaling of lengths and  $h$ . This leads to the following differential recursion relations:

$$\frac{d\kappa}{dl} = \kappa \left[ -\eta + g_1 - \frac{5}{2}g_2 \right], \quad (9)$$

$$\frac{dg_1}{dl} = g_1 \left[ \epsilon - \frac{5g_1}{2} + 5g_2 \right], \quad (10)$$

$$\frac{dg_2}{dl} = g_2 \left[ \epsilon - 4g_1 + \frac{15}{2}g_2 \right], \quad (11)$$

where  $\kappa(l=0) = \kappa_0$ , and we have defined two effective coupling constants,

$$g_1 \equiv \frac{AS_D k_B T \Lambda^{-\epsilon}}{(2\pi)^D \kappa^2}, \quad g_2 \equiv \frac{B^2 S_D k_B T \Lambda^{-\epsilon}}{(2\pi)^D \kappa^3}, \quad (12)$$

with  $A \equiv \frac{4\mu(\mu+\lambda)}{2\mu+\lambda} > 0$  and  $B \equiv \frac{2\chi\mu}{2\mu+\lambda}$ . Here,  $\exp(l)$  is the length rescaling factor,  $\epsilon \equiv 4 - D$ , where  $D$  is the "internal" dimension of the membrane (e.g.,  $D=2$  in the physical case), and  $S_D$  is the surface area of a  $D$ -dimensional sphere of unit radius. The flows in the  $g_1$ - $g_2$  plane are illustrated in Fig. 3.

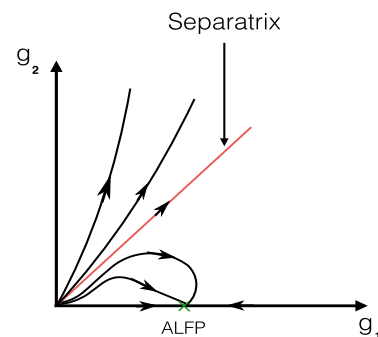


FIG. 3. (Color online) Schematic flow lines in the  $g_1 - g_2$  plane. (Green) cross marks the stable FP ( $2\epsilon/5, 0$ ). The red straight line is the separatrix  $g_2 = 3g_1/5$ .

As can be seen from that figure, the only stable fixed point is at  $g_2 = 0$ ,  $g_1 = 2\epsilon/5$ , which we will denote by call "ALFP" (Aronovitz-Lubensky fixed point) hereafter [13]. Since only  $g_2$  (which depends on  $B$ , and hence  $\chi$ ) and  $C$  involve any parameter that breaks the up-down symmetry of the lattice, the vanishing of  $g_2$  at the fixed

point implies that the large scale properties of any system whose starting parameters lie in the basin of attraction of this fixed point (i.e., the region below the separatrix in Fig. 3) will, with increasing length scale, become identical to those of a symmetric membrane, until we reach length scales at which  $C$  becomes important. Membranes in this region of parameter space are in the spiral state discussed below, whereas membranes whose bare  $g_{1,2}$  lie above the separatrix  $g_2 = 3g_1/5$  are crumpled, as we will discuss later.

We now turn to the effects of thermal fluctuations on the spiral phase itself. This requires studying the system at larger scales  $L \gg L_H$ . We still expect a double spiral (see Fig. 1) when  $T > 0$ . Thermal fluctuations open up the spiral by giving rise to a longer ranged "Helfrich repulsion"  $\mathcal{U}_H(d)$  [15, 16] that is caused by excluded volume interactions between parts of neighboring turns of the membrane that have made large excursions from their mean position (here  $d$  is the local mean separation between successive turns [17]). This interaction has the same form and scaling as for a lamellar phase of *symmetric* membranes [16], since  $g_2 \rightarrow 0$  upon renormalization below the separatrix, as discussed above. As shown in detail in the ALP, the result of balancing this interaction against the spontaneous curvature energy is the form of the spiral given by equations (2), (3), and (4). Note that this spiral phase displays orientational LRO.

Having discussed the spiral phase, we turn now to the other region of parameter space, namely that which flows away from the ALFP, and towards negative  $\kappa$ . While we cannot follow these flows all the way to  $\kappa = 0$  (since both  $g_{1,2}$  diverge there, so that our perturbation theory breaks down), we suspect that this signals crumpling of large membranes. This region of parameter space therefore corresponds to the crumpled phase. For  $\epsilon = 4 - D \ll 1$ , which is the region in which our perturbative RG is accurate, this is the region in figure (2) lying above the separatrix  $g_2 = 3g_1/5$ . For the physical case  $\epsilon = 2$ , as discussed in the ALP, it seems reasonable to assume that there continues to be a separatrix which, for small  $g_{1,2}$ , is a straight line  $g_2 = \rho g_1$  of universal slope  $\rho = \mathcal{O}(1)$ , although since  $\epsilon = 2$  we cannot calculate the universal constant  $\rho$ .

The range of  $\chi$  in our original model (5) that we are now discussing is  $\chi_L^2 < \chi^2 < \chi_U^2$ , where the upper bound follows because we are considering positive  $\kappa_0$  in Eq. (7), while the lower bound follows from assuming that we are above the separatrix, which implies, for small bare  $g_{1,2}^0$ , that  $g_2^0/g_1^0 > \rho$ . Using our earlier expressions (12) for  $g_{1,2}$ , we see that this implies

$$\chi^2 > \frac{\rho \kappa' (2\mu_0 + \lambda_0)}{\rho + \frac{\mu_0}{\mu_0 + \lambda_0}} = \frac{\chi_U^2}{1 + \frac{\mu_0}{\rho(\mu_0 + \lambda_0)}} \equiv \chi_L^2, \quad (13)$$

where in the equality we have used our result (8) for  $\chi_u^2$ . Note that, reassuringly, we always have  $\chi_L^2 < \chi_U^2$ , since  $\rho$ ,

$\mu_0$ , and  $\mu_0 + \lambda_0$  are all positive, the latter two positivities being required for stability.

For  $\chi$ 's in the range  $\chi_L^2 < \chi^2 < \chi_U^2$ , the membrane can remain uncrumpled if it is sufficiently small. This is because, in this range of  $\chi$ 's, the bare value  $\kappa(\ell = 0) = \kappa_0 = \kappa' - \frac{\chi^2}{2\mu_0 + \lambda_0}$ , is positive, and can stabilize orientational order and thereby prevent crumpling. Hence, that order will only be lost on length scales  $L > \xi$ , where  $\xi$  is the smallest length scale big enough to allow enough renormalization group "time"  $\ell$  for  $\kappa(\ell)$  to be driven to zero. This implies that the membrane will crumple unless new physics beyond the purely elastic model (5) intervenes on some length scale smaller than  $\xi$ .

Now we need to consider what "new physics" beyond the elastic model (5) can intervene before this length scale is reached to prevent crumpling. One possibility is self-avoidance, which can cut off any tendency to crumpling in the spiral sections of the membrane. But as inspection of figure (1) makes clear, this cut off cannot work for the straight section connecting the two oppositely returning spirals. This section has no neighbors, because it lies outside both spirals. It is therefore the section of the membrane that will crumple first, thereby inducing crumpling of the rest of the membrane.

This straight, "connecting" section of the membrane is stabilized by surface tension, which arises because that section of the membrane could lower its energy by "rolling up" into one or the other of the spiral sections it connects. It is not rolled up, of course, because the other spiral pulls it equally hard in the opposite direction. These two pulls create a non-zero surface tension  $\sigma$ , whose magnitude should be comparable to the Helfrich interaction in outermost turn of spiral, since it is the balance between that interaction, which works to open the spiral, and the spontaneous curvature term, which tries to tighten it, that sets the scale of that spontaneous curvature energy, and, hence, the surface tension. In the ALP we use this reasoning to calculate this surface tension  $\sigma$ , and the associated length scale  $L_\sigma = \sqrt{\frac{\kappa}{\sigma}}$  obtained by equating  $\sigma$  to the bending energy  $\frac{\kappa_0}{L_\sigma^2}$ . Equating  $L_\sigma$  to  $\xi$  and solving for  $L_m$  gives the maximum size  $L_c$  of the membrane that can be stable:

$$L_c \sim \frac{\kappa_0^{7/2} C_0^2}{(k_B T)^{5/2} B_0^3} \propto (\chi_U^2 - \chi^2)^{7/2}, \quad (14)$$

where the final proportionality follows from our expression (7) for  $\kappa_0$ . See Figs. 2 for schematic phase diagrams in the  $\chi - \kappa'$  and  $\chi^2 - L$  planes.

This scaling law breaks down both near  $\chi_U$ , where  $L_c$  gets to be  $R_s$ , so the membrane is not long enough to wind up at all, and as  $\chi \rightarrow \chi_L$ , for reasons discussed in the ALP.

*Summary:* We have developed the theory of asymmetric tethered membranes. This theory predicts a spiral

state, with the shape of the membrane at  $T = 0$  a double Archimedes spiral at  $T = 0$ , and an algebraic spiral with a universal exponent at  $T > 0$ . We also find that sufficiently asymmetric membranes are crumpled; the mechanism for this is quite different from “buckling” of elastic shells [18]. This leads to the phase diagrams (2), which can be tested in non living (ATP-depleted) RBC membrane extract [8], for model asymmetric membranes by binding spectrin to lipids [19], or graphene coated with some substance (e.g., polymer or a layer of lipid) on one side, as well as by numerical simulations [4, 20, 21]. We hope our work will stimulate experimental and numerical studies of asymmetric tethered membranes.

*Acknowledgements:-* T.B. and A.B. thank the Alexander von Humboldt Stiftung (Germany) for partial financial support under the Research Group Linkage Programme scheme (2016). T.B. and J. T. thank the Max-Planck Institut für Physik Komplexer Systeme, Dresden, Germany, for their hospitality and financial support while this work was underway.

---

\* [tirthankar.banerjee@u-psud.fr](mailto:tirthankar.banerjee@u-psud.fr)

† [niladri2002in@gmail.com](mailto:niladri2002in@gmail.com)

‡ [jjt@uoregon.edu](mailto:jjt@uoregon.edu)

§ [abhik.basu@saha.ac.in](mailto:abhik.basu@saha.ac.in), [abhik.123@gmail.com](mailto:abhik.123@gmail.com)

- [1] D. R. Nelson, T. Piran, and S. Weinberg, *Statistical mechanics of membranes and surfaces* (World Scientific, 2004).
- [2] M. E. Cates, “Statics and dynamics of polymeric fractals,” *Phys. Rev. Lett.* **53**, 926–929 (1984).
- [3] M. E. Cates, “The fractal dimension and connectivity of random surfaces,” *Phys. Lett. B* **161**, 363–367 (1985).
- [4] Y. Kantor, M. Kardar, and D. R. Nelson, “Tethered surfaces: Statics and dynamics,” *Phys. Rev. A* **35**, 3056 (1987).
- [5] M. Paczuski, M. Kardar, and D. R. Nelson, “Landau theory of the crumpling transition,” *Phys. Rev. Lett.* **60**, 2638–2640 (1988).
- [6] N. D. Mermin and H. Wagner, “Absence of ferromagnetism or antiferromagnetism in one-or two-dimensional isotropic heisenberg models,” *Phys. Rev. Lett.* **17**, 1133 (1966).
- [7] P. C. Hohenberg, “Existence of long-range order in one and two dimensions,” *Phys. Rev.* **158**, 383 (1967).
- [8] I. López-Montero, R. Rodríguez-García, and F. Monroy, “Artificial spectrin shells reconstituted on giant vesicles,” *J. Phys. Chem. Lett.* **3**, 1583–1588 (2012).
- [9] P. Le Doussal and L. Radzihovsky, “Self-consistent theory of polymerized membranes,” *Phys. Rev. Lett.* **69**, 1209 (1992).
- [10] L. Peliti and S. Leibler, “Effects of thermal fluctuations on systems with small surface tension,” *Phys. Rev. Lett.* **54**, 1690 (1985).
- [11] T. Banerjee, N. Sarkar, J. Toner, and A. Basu, “Statistical mechanics of asymmetric tethered membranes: spiral and crumpled phases,” companion long paper (2018).
- [12] P. M. Chaikin and T. C. Lubensky, *Principles of condensed matter physics* (Cambridge university press, 2000).
- [13] J. A. Aronovitz and T. C. Lubensky, “Fluctuations of solid membranes,” *Phys. Rev. Lett.* **60**, 2634 (1988).
- [14] S. Leibler, “Curvature instability in membranes,” *J. Physique* **47**, 507–516 (1986).
- [15] W. Helfrich, “Steric interaction of fluid membranes in multilayer systems,” *Z. Naturforsch. A* **33**, 305–315 (1978).
- [16] J. Toner, “New phase of matter in lamellar phases of tethered, crystalline membranes,” *Phys. Rev. Lett.* **64**, 1741 (1990).
- [17] Here by “local mean”, we mean the separation averaged over a “local” region small enough to look like a stack of parallel, flat membranes; this means the averaging volume must have a linear extent much less than the local radius of curvature, but much greater than the distance  $L_H$  between successive membrane contacts.
- [18] A. Košmrlj and D. R. Nelson, “Statistical mechanics of thin spherical shells,” *Phys. Rev. X* **7**, 011002 (2017).
- [19] P. J. O’Toole, I. E. G. Morrison, and R. J. Cherry, “Investigations of spectrin–lipid interactions using fluoresceinphosphatidylethanolamine as a membrane probe,” *Biochimica et Biophysica Acta (BBA)-Biomembranes* **1466**, 39–46 (2000).
- [20] F. F. Abraham, W. E. Rudge, and M. Plischke, “Molecular dynamics of tethered membranes,” *Phys. Rev. Lett.* **62**, 1757 (1989).
- [21] Z. Peng, X. Li, I. V. Pivkin, M. Dao, G. E. Karniadakis, and S. Suresh, “Lipid bilayer and cytoskeletal interactions in a red blood cell,” *Proc. Nat. Acad. Sc. (USA)* **110**, 13356–13361 (2013).